shown to be exclusively localized in caveolar membrane fractions (Fig. 4B), which is characteristic of dynamic clustering of sphingolipids and cholesterol (*28, 29*). Treatment of the cells by filipin, which disperses caveolar domains (*30*), resulted in a dose-dependent inhibition of Stat1 activation (*16*), and this inhibition was reversible (Fig. 4C), suggesting that the localization of IFNGR and IFNAR is critical for efficient signaling. The intracellular levels of Jak1 and Jak2 were also found to be concentrated in the caveolar membrane domains (Fig. 4B), suggesting that the caveolar domain–dependent signaling may be a feature shared by other cytokines that use these kinases for signaling. Local concentration of cytokine receptors at caveolar membrane may be important for efficient ligand-induced receptor oligomerization and cross talk among cytokine receptor components.

References and Notes

1. C. Weissmann and H. Weber, *Prog. Nucleic Acid Res. Mol. Biol.* **33**, 251 (1986).
2. E. DeMaeyer and J. DeMaeyer-Guignard, *Interferons and Other Regulatory Cytokines* (Wiley, New York, 1988).
3. J. Vilcek and G. S. Sen, in *Fields Virology*, D. M. Fields, P. M. Knipe, P. M. Howley, Eds. (Lippincott-Raven, Philadelphia, ed. 3, 1996), p. 375.
4. S. Pestka, J. A. Langer, K. C. Zoon, C. E. Samuel, *Annu. Rev. Biochem.* **56**, 727 (1987).
5. A. Billiau, *Adv. Immunol.* **62**, 61 (1996).
6. C. Schindler and J. E. Darnell Jr., *Annu. Rev. Biochem.* **64**, 621 (1995).
7. E. A. Bach, M. Aguet, R. D. Schreiber, *Annu. Rev. Immunol.* **15**, 563 (1997).
8. G. R. Stark, I. M. Kerr, B. R. Williams, R. H. Silverman, R. D. Schreiber, *Annu. Rev. Biochem.* **67**, 227 (1998).
9. J. E. Darnell Jr., I. M. Kerr, G. R. Stark, *Science* **264**, 1415 (1994).
10. J. N. Ihle and I. M. Kerr, *Trends Genet.* **11**, 69 (1995).
11. A. R. Bluyssen, J. E. Durbin, D. E. Levy, *Cytokine Growth Factor Rev.* **7**, 11 (1996).
12. The result of the antiviral assay presented in figure 2A of U. Müller et al. [*Science* **264**, 1918 (1994)] is consistent with our present results. To investigate further the extent to which the loss of IFNAR1 affects IFN-γ–induced gene expression, we examined the mRNA induction kinetics for *IRF-1* and *2′,5′OAS* genes by IFN-γ in the WT and IFNAR1-null MEFs. The induction of IRF-1 mRNA by IFN-γ was six times lower in the mutant MEFs than in the WT MEFs. We also examined the induction of *2′,5′OAS* mRNA, which is dependent on ISGF3, in the WT and IFNAR1-null MEFs. The induction of *2′,5′OAS* mRNA by IFN-γ remained undetectable in IFNAR1-null MEFs throughout the time course tested (*19*).
13. S. Huang et al., *Science* **259**, 1742 (1993).
14. IFNAR1-deficient and IFNGR1-deficient mice were purchased from B&K Universal Group (North Humberside, UK). MEFs and splenocytes were prepared according to standard methods [A. Takaoka et al., *EMBO J.* **18**, 2480 (1999)]. Recombinant murine IFN-γ was purchased from Genzyme/Techne.
15. Flow cytometry and immunoblot analyses revealed that the expression levels of IFNGR1 and IFNGR2 in these cells are essentially the same as in the WT MEFs. Immunoblot analysis showed that nearly the same amount of endogenous Stat1 protein was detected in the WT and IFNAR1-null MEFs.
16. A. Takaoka and Y. Mitani, unpublished data.
17. M. Matsumoto et al., *Biol. Chem.* **380**, 699 (1999).
18. T. Kimura et al., *Genes Cells* **1**, 115 (1996).
19. Supplemental Web material is available at *Science* Online at www.sciencemag.org/feature/data/1049334.shl.
20. M. Sato, unpublished results.
21. L. Erlandsson et al., *Curr. Biol.* **8**, 223 (1998).
22. K. Shuai et al., *Cell* **76**, 821 (1994).
23. X. Li, S. Leung, I. M. Kerr, G. R. Stark, *Mol. Cell. Biol.* **17**, 2048 (1997).
24. H. Yan et al., *EMBO J.* **15**, 1064 (1996).
25. A. C. Greenlund, M. A. Farrar, B. L. Viviano, R. D. Schreiber, *EMBO J.* **13**, 1591 (1994).
26. W. R. Fleischmann Jr., J. A. Georgiades, L. C. Osborne, H. M. Johnson, *Infect. Immun.* **26**, 248 (1979).
27. W. E. Stewart II, L. B. Gosser, R. Z. Lockart Jr., *J. Virol.* **7**, 792 (1971).
28. K. Simons and E. Ikonen, *Nature* **387**, 569 (1997).
29. R. Xavier, T. Brennan, Q. Li, C. McCormack, B. Seed, *Immunity* **8**, 723 (1998).
30. Detergent-free caveolae fractions were prepared as described [E. J. Smart, Y. S. Ying, C. Mineo, R. G. Anderson, *Proc. Natl. Acad. Sci. U.S.A.* **92**, 10104 (1995); C. Mineo, G. L. James, E. J. Smart, R. G. Anderson, *J. Biol. Chem.* **271**, 11930 (1996)]. The reversibility of the effects of filipin treatment was investigated as described [J. E. Schnitzer, P. Oh, E. Pinney, J. Allard, *J. Cell. Biol.* **127**, 1217 (1994); R. Xavier, T. Brennan, Q. Li, C. McCormack, B. Seed, *Immunity* **8**, 723 (1998)]. Briefly, MEFs treated with filipin (Sigma) for 10 min were washed, incubated for 60 min in Dulbecco's modified Eagle's medium containing 20% fetal calf serum, and then stimulated with IFN-γ.
31. M. Sato et al., *FEBS Lett.* **441**, 106 (1998).
32. A. Takaoka et al., *EMBO J.* **18**, 2480 (1999).
33. Preparation of whole-cell extracts, binding reactions, and gel electrophoresis were done as described [A. Takaoka et al., *EMBO J.* **18**, 2480 (1999)]. Unless otherwise noted, cells were treated with IFN-γ (250 U/ml) for 30 min. Equal amounts of proteins from whole-cell extracts were loaded onto each lane. Experiments were done in triplicate and were performed separately with at least two independent clones of MEFs derived from the same littermates of the WT or mutant mice.
34. After the treatment with IFN-γ (250 U/ml) for 15 min, cell lysis, immunoprecipitation, and immunoblotting were done as described [A. Takaoka et al., *EMBO J.* **18**, 2480 (1999)]. The following antibodies were purchased: anti-phosphotyrosine, anti-Jak1, and anti-Jak2 (Upstate Biotechnology); anti-Stat1 p84/p91 and anti-Stat2 (Santa Cruz); anti-phosphorylated Stat1 (Tyr⁷⁰¹) (New England BioLabs); anti-IFNAR1, anti-IFNGR1, and anti-IFNGR2 (Research Diagnostics); and anti-caveolin (Transduction Laboratories).
35. We thank G. Uzé for the murine IFNAR1 cDNA (GenBank accession number M89041); J. Vilcek and E. L. Barsoumian for invaluable advice; M. Asagiri, N. Hata, Y. Kato, and S. H. Kim for technical support; Sumitomo Pharmaceuticals for purified murine IFN-α; and Toray Industries for recombinant murine IFN-β. Animal care was in accordance with institutional guidelines of the University of Tokyo. Supported by grants from the Research for the Future Program (96L00307), Yamanouchi Foundation for Research on Metabolic Disorders, the Japan Society for the Promotion of Science, Advanced Research on Cancer, and the Human Frontier Science Program Organization.

Perception of Brassinosteroids by the Extracellular Domain of the Receptor Kinase BRI1

**Zuhua He,[1,3,4] Zhi-Yong Wang,[1] Jianming Li,[1]* Qun Zhu,[1]†
Chris Lamb,[1]‡ Pamela Ronald,[3] Joanne Chory[1,2]§**

An assay was developed to study plant receptor kinase activation and signaling mechanisms. The extracellular leucine-rich repeat (LRR) and transmembrane domains of the *Arabidopsis* receptor kinase BRI1, which is implicated in brassinosteroid signaling, were fused to the serine/threonine kinase domain of XA21, the rice disease resistance receptor. The chimeric receptor initiates plant defense responses in rice cells upon treatment with brassinosteroids. These results, which indicate that the extracellular domain of BRI1 perceives brassinosteroids, suggest a general signaling mechanism for the LRR receptor kinases of plants. This system should allow the discovery of ligands for the LRR kinases, the largest group of plant receptor kinases.

Receptor kinases mediate extracellular signals for diverse processes in plants and animals. Detailed mechanistic studies of both receptor tyrosine kinases and receptor serine/threonine kinases have been well documented in animal cells, where it has been shown that ligand binding to the extracellular domains of receptors induces receptor dimerization and stimulates receptor phosphorylation, resulting in the activation of intracellular signaling cascades (*1–3*). In contrast, the study of plant receptor-like kinases (RLKs), all of which are serine/threonine kinases, is still in its infancy (*4, 5*). Despite the large numbers of putative RLKs encoded in the genomes of plants, how these receptors carry out signal transduction has yet to be determined.

Of the various RLKs, the largest group is the leucine-rich repeat receptor kinases (LRR-RLKs). This class consists of at least 120 genes in *Arabidopsis*. A few LRR-RLKs are involved in diverse biological processes based on their

[1]Plant Biology Laboratory, [2]The Howard Hughes Medical Institute, The Salk Institute for Biological Studies, La Jolla, CA 92037, USA. [3]Department of Plant Pathology, University of California, Davis, CA 95616, USA. [4]Biotechnology Institute, Zhejiang University, Hangzhou 310029, China.

*Present address: Department of Biology, University of Michigan, MI 48190−1048, USA.
† Present address: Dupont Company, Wilmington, DE 19880−0402, USA.
‡ Present address: John Innes Centre, Norwich, NR4 7UH, UK.
§To whom correspondence should be addressed. E-mail: chory@salk.edu

mutant phenotypes. These processes include the control of meristem development (*6*), disease resistance (*7*), hormone signaling (*8*), and organ elongation and abscission (*9, 10*). However, in no case is there biochemical evidence for the identity of a ligand, although genetic studies have provided some clues. On the basis of the similarity of mutant phenotypes and their adjacent expression domains within the meristem, CLAVATA3, a putative extracellular protein of 96 amino acids, has been proposed as the ligand of the LRR-RLK CLAVATA1 (*11*). Likewise, genetic studies suggest that the steroid hormone brassinolide (BL), the most biologically active brassinosteroid, is the ligand for the *BRI1*-encoded LRR-RLK (*8*). Thus, the LRR-RLKs might use either small molecules or proteins as ligands.

To determine if BRI1 plays a direct role in BL perception, we developed a cell-based assay using the XA21 LRR-RLK from rice. XA21 confers resistance to *Xanthomonas oryzae* pv. *oryzae* (*Xoo*) (*7*). Most incompatible plant/pathogen interactions lead to a hypersensitive response (HR) that includes an oxidative burst, defense gene activation, and cell death (*12, 13*). Thus, XA21 signaling outputs may provide a facile assay for determining the mechanism of LRR-RLK signaling. Figure 1 shows that stably transformed *O. sativa* ssp. *Japonica* var. Taipei 309 cells expressing full-length XA21 from its native promoter exhibit race-specific defense responses (*14*). XA21 expression initiated cell death in lines that were inoculated with the incompatible *Xoo* Phillipine Race 6 (P6) strain PXO99A, but not when inoculated with the compatible Korean Race 1 (K1) strain DY89031 (Fig. 1A).

Pathogen-induced cell death is often accompanied by an oxidative burst (*13*). A small, but highly reproducible oxidative burst was observed in the XA21 cell line inoculated for 1 hour with the incompatible P6, compared with inoculation with the compatible K1 strain (Fig. 1B). This small increase of H_2O_2 levels, although not as large as those reported for other plants, is consistent with the levels of H_2O_2 that we have seen in rice (*15*).

Activation of XA21 signaling leads to rapid and strong induction of transcription of the rice defense genes chitinase *RCH10* (*16*) and phenylalanine ammonia-lyase (*PAL*) (*17*) in the incompatible interaction with *Xoo* (Fig. 1, C and D), whereas the compatible interaction shows a weaker and slower accumulation of these transcripts. This race-specific difference correlates to whole plant assays (*18*). The expression of a rice catalase B gene (*OsCatB*) (*19*) was strongly down-regulated in the XA21 cell line inoculated with the incompatible strain (Fig. 1, C and D), as seen in whole plants (*20*). Taken together, these results establish the rice cell culture system as an excellent reporter of the signaling output of LRR-RLKs.
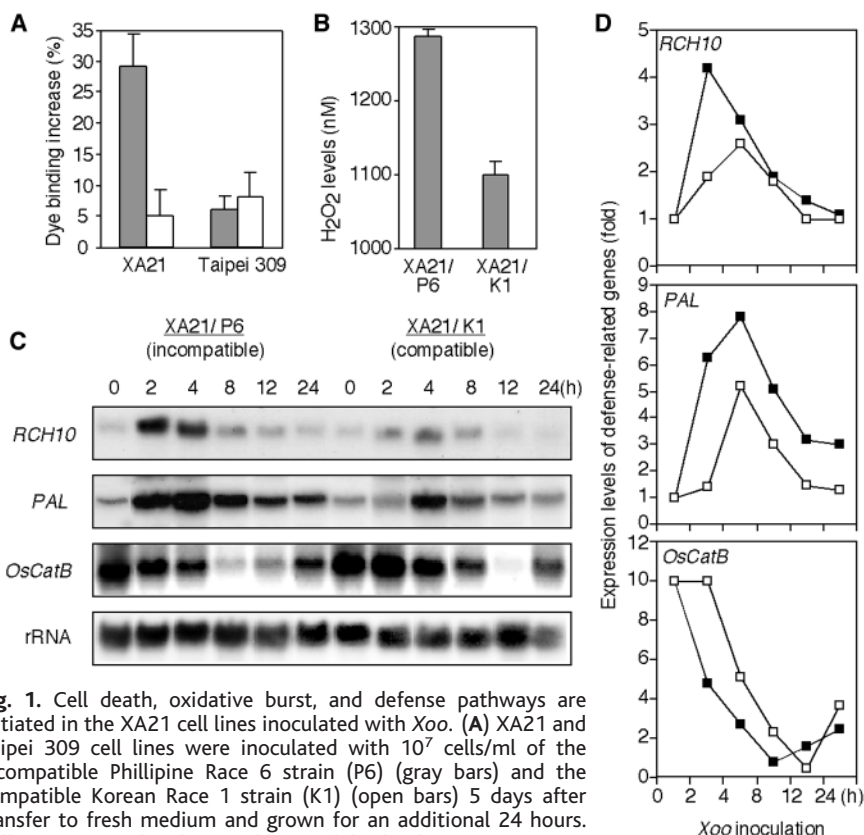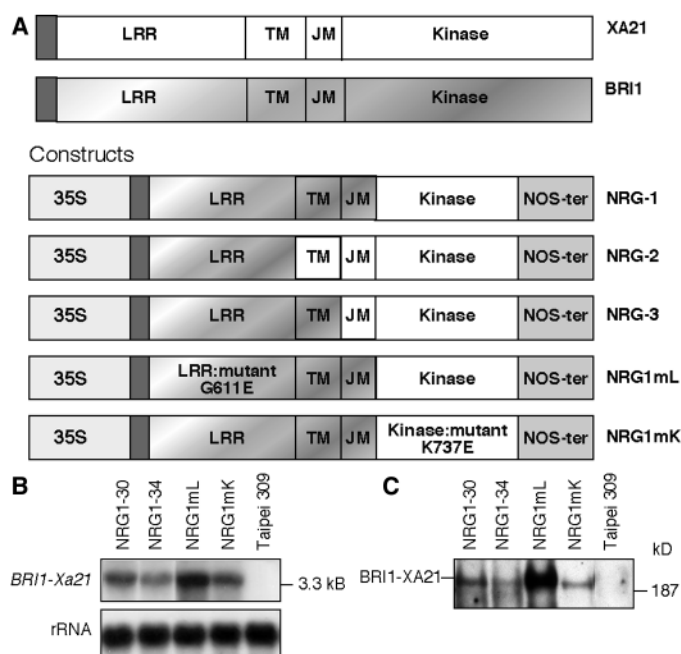

Fig. 1. Cell death, oxidative burst, and defense pathways are initiated in the XA21 cell lines inoculated with *Xoo*. (**A**) XA21 and Taipei 309 cell lines were inoculated with 10^7 cells/ml of the incompatible Phillipine Race 6 strain (P6) (gray bars) and the compatible Korean Race 1 strain (K1) (open bars) 5 days after transfer to fresh medium and grown for an additional 24 hours. Cells were stained with Evans blue, and dye binding increases over uninoculated controls were quantified as an indicator of cell death. The experiment was repeated five times. (**B**) Cells were inoculated for 1 hour with P6 and K1 (10^7 cells/ml). H_2O_2 levels in media were assayed (*23*) with at least three repeats. (**C**) Northern blotting shows changes in the expression of defense genes *RCH10*, *PAL*, and *OsCatB* over a time course of 0 to 24 hours after *Xoo* inoculation (*24*). (**D**) mRNA levels were estimated with a PhosphoImager System (Molecular Dynamics, Sunnyvale, California). Levels at time 0 were set as onefold for *RCH10* and *PAL* and 10-fold for *OsCatB*. Curves indicate incompatible (■) and compatible (□) interactions.

Fig. 2. (**A**) Schematic diagram of chimeric receptor kinases NRG1, NRG2, and NRG3 and mutant controls NRG1mL and NRG1mK. The XA21 and BRI1 protein structures are labeled in white and gray, respectively, with signal peptides indicated in dark gray. These chimeras were constructed by in vitro mutagenesis (*25*) and driven by the cauliflower mosaic virus 35S promoter in rice cells (*9*) (**B**) Northern hybridization shows mRNA accumulation of each chimeric gene, with a 1.3-kb DNA fragment of the *Xa21* kinase domain as a probe. (**C**) Western blot shows the expression of BRI1-XA21 chimeric proteins (*26*).

To test the mechanism by which BRI1 signals, we constructed several chimeric receptors between BRI1 and XA21 (Fig. 2; NRG1, NRG2, and NRG3). Of the three receptors, only one, NRG1, consisting of BRI1's extracellular and transmembrane domains and 65 amino acids of the intracellular domain (juxtamembrane domain) fused to the kinase domain of XA21, was able to elicit the HR (Figs. 2 and 3, discussed below). As controls, we also constructed mutant versions of the NRG1 chimeric receptor. Previous studies have implicated the importance of a 70–amino acid island embedded between the 21st and 22nd LRR of BRI1's extracellular domain for BRI1 function (8). One naturally occurring allele of *BRI1*, *bri1-113*, is a mutation of glycine at position 611 in this domain to glutamate (Gly^{611} → Glu). The mutant chimeric receptor, NRG1mL, incorporates this change into the NRG1 construct. We also constructed a kinase domain mutant of XA21 (Lys^{737} → Glu) in the chimeric receptor NRG1mK, which lacks kinase activity in vitro (19). Transgenic cell lines were established by transforming the rice line Taipei 309 (14). Northern and Western blotting confirmed that two of the NRG1-expressing lines, NRG1-30 and NRG1-34, and the mu-

tant receptor, NRG1mK, were expressed at comparable levels in the cell lines (Fig. 2, B and C). NRG1mL accumulated to higher levels (Fig. 2, B and C). Regenerated NRG1 transgenic plants were dwarfed and sterile and exhibited partial resistance to *Xoo* after BL treatment as compared with controls (15).

We found that NRG1 could initiate the HR upon addition of BL using two different cell lines, NRG1-30 and NRG1-34 (Fig. 3). Cell death was observed after treatment for 24 hours with 2 μM BL (Fig. 3A), whereas very little cell death occurred in the Taipei 309 control, NRG1mL (Gly^{611} → Glu), or NRG1mK (Lys^{737} → Glu) cells. The magnitude of increase in cell death was comparable to that seen in the incompatible pathogen-XA21 interaction (Fig. 1A). Likewise, we observed a detectable oxidative burst in the NRG1 cell lines within 30 min of BL treatment (Fig. 3B). Changes in expression of defense genes were monitored in the wild-type and mutant receptor lines (Fig. 3, C and D). We observed an accumulation of both *RCH10* and *PAL* mRNAs in response to 2 μM BL in both NRG1 lines, with peak levels (five- to eightfold) occurring 4 to 8 hours after BL treatment (Fig. 3, C and D). In contrast, neither NRG1mL, NRG1mK, nor the Taipei 309 control cells showed an induction of

RCH10 or *PAL* mRNAs (Fig. 3, C and D). Accumulation of *OsCatB* RNA was inhibited in NRG1-30 and NRG1-34 cell lines 2 to 12 hours after BL treatment (Fig. 3, C and D). We did not detect cell death in transgenic cell lines carrying the XA21 wild-type protein or overexpressing the XA21 kinase domain after BL treatment (15).

A BL dose-response curve was constructed with *RCH10* RNA accumulation as a reporter. We saw *RCH10* induction using concentrations of BL as low as 10 nM; the response began to saturate at about 2 μM BL (Fig. 4). These BL concentrations are physiologically relevant, being consistent with those for rescue of the *Arabidopsis* BL biosynthetic mutant, *det2* (21). These three assays indicate that the BRI1-XA21 chimeric receptor can recognize BL to activate cell death, the oxidative burst, and defense gene induction. Moreover, both the extracellular/transmembrane/juxtamembrane domains of BRI1 and the XA21 kinase domain are required for these responses.

Our studies indicate that BRI1 plays a direct role in brassinosteroid perception and that the response is cell autonomous. We have recently shown that BRI1 is a ubiquitously expressed, plasma membrane–localized protein (22). Thus, our data provide strong evidence that plant steroids are perceived at the cell surface. Moreover, the observation that a mutation in the 70–amino acid island region of the extracellular domain of BRI1 results in a receptor that cannot perceive BL reinforces the notion that this region is important for steroid binding or proper folding of the extracellular domain for BL recognition.
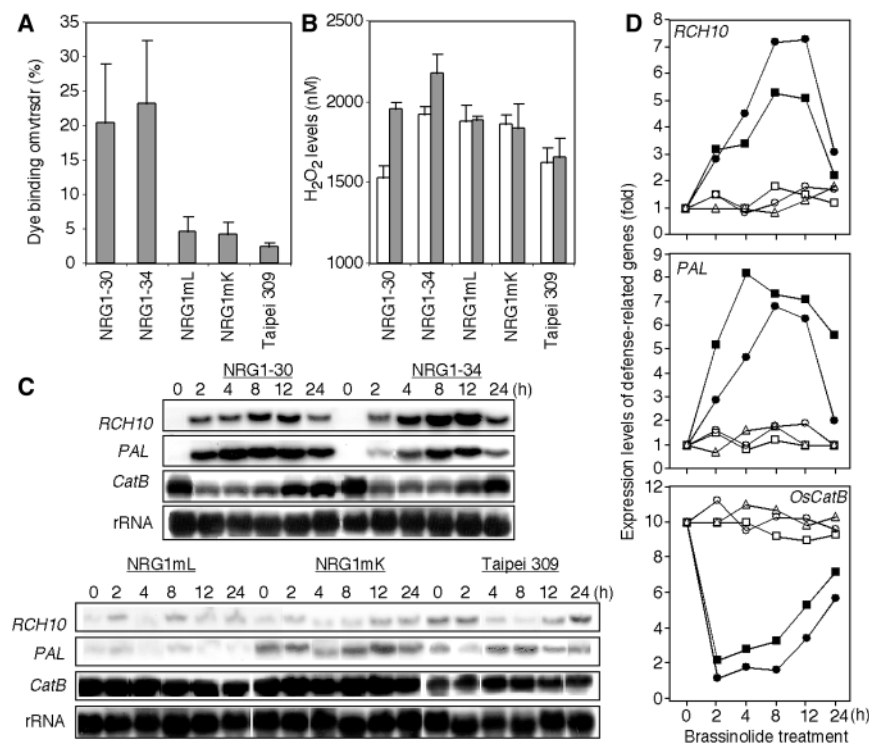

Fig. 3. BL induces cell death, oxidative burst, and defense pathway activation in NRG1 cell lines. (**A**) Cell suspensions (14): NRG1-30, NRG1-34, NRG1mL, NRG1mK, and wild-type Taipei 309 were treated with 2 μM BL for 24 hours. Cell death was assayed as described in Fig. 1A. (**B**) NRG1 and control cell lines were treated for 30 min with 2 μM BL for H$_2$O$_2$ production assay (23), with gray bars for treatment and open bars for nontreatment. (**C**) Cell lines were treated with 2 μM BL for 0 to 24 hours. Transcript accumulation of defense-related genes *RCH10*, *PAL*, and *OsCatB* was determined by Northern blotting (24). (**D**) RNA levels were estimated as in Fig. 1D. Cell lines are NRG1-30 (■), NRG1-34 (●), NRG1mL (□), NRG1mK (○), and Taipei 309 (△).
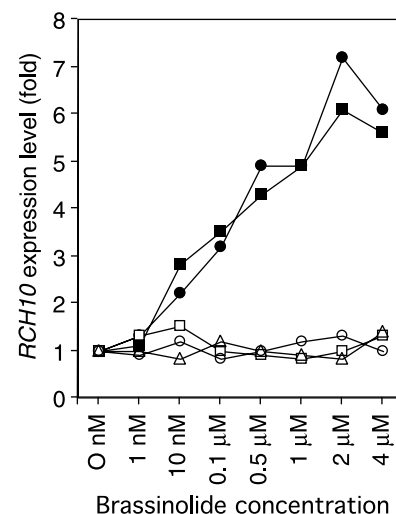
Fig. 4. BL dose response for *RCH10* induction in *NRG1* cell lines. Cells were treated with 0 to 4 μM BL. RNA was extracted 6 hours after treatment, and transcript levels were determined (24). Cell lines are NRG1-30 (■), NRG1-34 (●), NRG1mL (□), NRG1mK (○), and Taipei 309 (△).

These results suggest a mechanism of signaling conserved between BRI1 and XA21 that may be extrapolated to the large number of LRR-RLKs found in plant genomes. The model would include ligand perception through the extracellular/transmembrane domain, whereas the intracellular kinase domain determines the downstream signaling response. There are greater than 120 LRR-RLKs predicted in the *Arabidopsis* genome sequencing project. The chimeric receptor approach, using the XA21 signaling outputs defined here, should provide an assay system that is applicable to the discovery of ligands for the LRR-RLKs, as well as aid in the design of novel signaling genes for controlling plant development and disease resistance.

References and Notes

1. P. van der Geer, T. Hunter, R. Lindberg, *Annu. Rev. Cell Biol.* **10**, 251 (1994).
2. J. Massagué, *Cell* **85**, 947 (1996).
3. X. Feng and R. Deryneck, *EMBO J.* **16**, 3912 (1997).
4. K. Lease, E. Ingham, J. C. Walker, *Curr. Opin. Plant Biol.* **1**, 388 (1998).
5. P. Becraft, *Trends Plant Sci.* **3**, 384 (1998).
6. S. Clark, R. Williams, E. Meyerowitz, *Cell* **89**, 575 (1997).
7. W. Song et al., *Science* **270**, 1804 (1995).
8. J. Li and J. Chory, *Cell* **90**, 92 (1997).
9. K. Torii et al., *Plant Cell* **8**, 735 (1996).
10. T. L. Lin, J. Stone, J. Walker, *Genes Dev.* **14**, 108 (2000).
11. J. Fletcher, U. Brand, M. Running, R. Simon, E. Meyerowitz, *Science* **283**, 1911 (1999).
12. G. Martin, *Curr. Opin. Plant Biol.* **2**, 273 (1999).
13. A. Levine, R. Tenhaken, R. Dixon, C. Lamb, *Cell* **79**, 583 (1994).
14. Rice transformation was as described [L. Chen, S. Zhang, R. N. Beachy, C. M. Fauquet, *Plant Cell Rep.* **18**, 25 (1998)]. Cell suspension lines were established in NB6 medium from transformants. The XA21 cell line was established from homozygous seeds of XA21 transgenic line 106 (7).
15. Z. He and P. Ronald, unpublished data.
16. Q. Zhu and C. Lamb, *Mol. Gen. Genet.* **226**, 289 (1991).
17. Q. Zhu et al., *Plant Mol. Biol.* **29**, 535 (1995).
18. M. Yoshikawa and P. Ronald, unpublished data.
19. W. Song and P. Ronald, unpublished data.
20. S. Yi, S. Yu, D. Choi, *Mol. Cell* **9**, 320 (1999).
21. J. Li, P. Nagpal, V. Vitart, T. C. McMorris, J. Chory, *Science* **272**, 398 (1996).
22. D. Friedrichsen, C. Joazeiro, J. Li, T. Hunter, J. Chory, *Plant Physiol.*, in press.
23. After treatment, media were filtered to remove cells with 0.2-μm syringe filters. One hundred–microliter samples were added to 1 ml of reaction buffer [0.25 mM FeSO$_4$, 0.25 mM (NH$_4$)$_2$SO$_4$, 25 mM H$_2$SO$_4$, 1.25 μM xylenol orange, and 1 mM sorbitol] at room temperature for 1 hour. Absorbance was measured at 560 nm, and H$_2$O$_2$ levels were calculated by reference to standards [Z. Jiang, J. V. Hunt, S. P. Wolff, *Anal. Biochem.* **202**, 383 (1992)].
24. RNA was extracted from the XA21 cell lines at 0 to 24 hours after inoculation with P6 and K1 (10^7 cells per milliliter), with the TRIzol reagent (Life Technologies, Gaithersburg, MD). Thirty micrograms of total RNA was used in each lane. A 1.2-kb fragment of rice chitinase *RCH10* (13), a 400–base pair fragment of *PAL* (17), and a cDNA clone of *OsCatB* (19) were used as probes. The filters were reprobed with 18*S Arabidopsis* rDNA for normalization.
25. A *BRI1* DNA fragment encoding the presumed extracellular, transmembrane (TM), and juxtamembrane (JM) domains [amino acids 1 to 879 (8)] was fused with the *Xa21* fragment encoding the predicted kinase domain [amino acids 708 to 1025 (7)] to make NRG1. NRG2 consisted of amino acids 1 to 769 of BRI1 and the XA21 TM, JM, and kinase domains with amino acids 625 to 1025. NRG3 consisted of amino acids 1 to 834 of BRI1 and amino acids 684 to 1025 of XA21. NRG1mL contains a mutation (Gly^{611} → Glu) corresponding to the allele *bri1-113* (8). NRG1mK is a mutation of XA21 (Lys^{737} → Glu) obtained by in vitro mutagenesis with the primer (5'-GTTGCAGTGGAGGTACTAA-3') corresponding to the *Xa21* sequence 2197 to 2215 (7).
26. Cells were homogenized in 50 mM tris-HCl (pH 7.5), 200 mM mannitol, 10 mM MgCl$_2$, and protease inhibitor cocktail (Boehringer Mannheim). After centrifugation at 10,000*g* for 20 min, the supernatant was centrifuged at 100,000*g* for 1 hour to collect membranes. Membrane proteins (80 μg per lane) were resolved on a 3 to 8% gradient SDS-NuPAGE gel (Invitrogen), transferred to nitrocellulose, and probed with affinity-purified antibodies raised to BRI1's NH$_2$-terminal 106 amino acids.

Perception of Environmental Signals by a Marine Diatom

Angela Falciatore,[1] Maurizio Ribera d'Alcalà,[2] Peter Croot,[3] Chris Bowler[1]*

Diatoms are a key component of marine ecosystems and are extremely important for the biogeochemical cycling of silica and as contributors to global fixed carbon. However, the answers to fundamental questions such as what diatoms can sense in their environment, how they respond to external signals, and what factors control their life strategies are largely unknown. We generated transgenic diatom cells containing the calcium-sensitive photoprotein aequorin to determine whether changes in calcium homeostasis are used to respond to relevant environmental stimuli. Our results reveal sensing systems for detecting and responding to fluid motion (shear stress), osmotic stress, and iron, a key nutrient that controls diatom abundance in the ocean.

The predominance of diatoms in marine ecosystems indicates that they possess sophisticated strategies for responding to environmental variation. However, little is known about these strategies at the cellular level because of the difficulties of monitoring key internal physiological processes in these organisms. The recent availability of procedures to generate transgenic diatoms (*1–3*) has opened up a range of techniques that can be used to address these questions.

We transformed the marine diatom *Phaeodactylum tricornutum* (*4*) with a construct containing the apoaequorin cDNA derived from the jellyfish *Aequorea victoria* (*5*). Transgenic cells displaying high levels of aequorin were selected (*4*) and used to analyze diatom responses to a range of different stimuli.

Transient changes in cytosolic calcium concentrations ($[Ca^{2+}]_{cyt}$), which are characteristic of the activation of signal transduction (*6*), could be observed in response to the sim- ple addition of seawater [artificial seawater (ASW)] (Fig. 1A). A maximal increase in $[Ca^{2+}]_{cyt}$ from 500 nM to 2 μM was observed after 1 to 2 s, which quickly disappeared within 10 s. This response weakened with declining stimulus strength (*7*). To exclude the possibility that chemical signaling may have been involved as a result of the addition of fresh medium to the cells, we confirmed that conditioned medium (medium in which the diatoms had been growing) was able to generate the same effects, as was the mechanical stimulation of the cell suspension with a needle (Fig. 1A). When these experiments were repeated with a pH microelectrode in the suspension, no changes in pH were detected after the treatments (*8*), thus excluding the possibility that the observed calcium responses were a consequence of external pH changes.

When organisms are exposed to a stimulus for a long enough period, they typically lose their ability to respond with their original sensitivity. By this process of short-term adaptation or desensitization, a cell reversibly adjusts its sensitivity to the level of the stimulus. At the molecular level, the best understood examples of adaptation occur in bacterial chemotaxis (*9*) and in photoperception in the retina (*10*). To determine whether diatoms possess such sophisticated sensing systems for responding to fluid motion, we examined the effect of giving

[1]Laboratories of Molecular Plant Biology and [2]Biological Oceanography, Stazione Zoologica Anton Dohrn, Villa Comunale, I-80121 Naples, Italy. [3]Department of Marine Chemistry and Geology, Netherlands Institute for Sea Research (NIOZ), Postbus 59, 1790 AB Den Burg, Texel, Netherlands.

*To whom correspondence should be addressed. E-mail chris@alpha.szn.it